

On the Wilson–Bappu relationship in the Mg II k line

A. Cassatella^{1,2}, A. Altamore², M. Badiali¹, and D. Cardini¹

¹ Istituto di Astrofisica Spaziale, CNR, Area di Ricerca Tor Vergata, Via del Fosso del Cavaliere 100, 00133 Roma, Italy

² Dipartimento di Fisica E. Amaldi, Università degli Studi Roma Tre, Via della Vasca Navale 84, 00146 Roma, Italy

Received 28 March 2001 / Accepted 5 June 2001

Abstract. An investigation is carried out on the Wilson–Bappu effect in the Mg II k line at 2796.34 Å. The work is based on a selection of 230 stars observed by both the *IUE* and *HIPPARCOS* satellites, covering a wide range of spectral types (F to M) and absolute visual magnitudes ($-5.4 \leq M_V \leq 9.0$). A semi-automatic procedure is used to measure the line widths, which applies also in the presence of strong central absorption reversal. The Wilson–Bappu relationship here provided is considered to represent an improvement over previous recent results for the considerably larger data sample used, as well as for a proper consideration of the measurement errors. No evidence has been found for a possible dependence of the WB effect on stellar metallicity and effective temperature.

Key words. stars: distances – stars: late-type – ultraviolet: general – line: profiles – catalogs

1. Introduction

Several papers have been devoted to the study of the correlation between the visual absolute magnitude M_V of intermediate and late-type stars, and the width of the Mg II k 2796.34 Å emission line (cf. Garcia–Alegre et al. 1981; Vladilo et al. 1987; Elgarøy 1988; Elgarøy et al. 1988; Scoville & Mena–Werth 1998, hereafter SMW; Elgarøy et al. 1999, hereafter EEL).

The width–luminosity relationship for the Mg II k line is qualitatively similar to the one found by Wilson & Bappu (1957) for the Ca II k optical line (see also recent work by Wallerstein et al. 1999), currently known as the Wilson–Bappu effect (hereafter WB). Given the similar excitation conditions of these lines, the dependence of their line widths on stellar luminosity or on other fundamental stellar parameters rests on the same physical processes. For a short review on models see Montes et al. (1994), references therein, and the recent work by Özeren et al. (1999).

In this paper we study the WB correlation for the Mg II k line using the widest possible sample of stars observed at high resolution with *IUE*, and having a reliable parallax determination from the *HIPPARCOS* experiment. More precisely, the purposes of the present paper are:

a) to refine the previous luminosity calibrations of the Mg II k line width by using an homogeneous set of mea-

surements of a statistically significant number of stars covering also spectral types and luminosity classes poorly represented in previous investigations. Particular care has been taken to properly consider the measurement errors; b) to clarify the problem of the possible dependence of the Mg II k line width on stellar effective temperature and metallicity discussed in previous papers.

Details about the definition of the present data sample, the observations, and the method used to measure the line widths are given in Sects. 2 and 3. The results and the conclusions are presented in Sects. 4 and 5, respectively.

2. The present sample of stars

A search for all stars with spectral types F, G, K and M with a known parallax from the *HIPPARCOS* experiment and observed at high resolution in the long wavelength camera by *IUE* provides 835 *IUE* spectra of 376 stars with a wide range of luminosity from main sequence to supergiants. From this initial sample we have purposely excluded some special classes of stars. Chromospherically active binary stars such as RS CVn and BY Dra stars were excluded since their Mg II profiles may be systematically broader than in non-active stars (Montes et al. 1994; Özeren et al. 1999). Mira variables and Cepheids were excluded because their *V* magnitudes and Mg II line profiles are variable and phase-dependent, and also because of the importance of shock waves associated with pulsation as a source of line excitation in these objects (see Gillet et al. 1985; Kraft 1960). Also excluded were binary stars having the Mg II lines broadened by peculiar processes (see for

Send offprint requests to: D. Cardini,
e-mail: cardini@ias.rm.cnr.it

example the case of the M-type giant Mira Ceti, in which the emission lines arise from an optically thin disk around the white dwarf companion, as reported by Cassatella et al. 1985 and Reimers & Cassatella 1985). Finally, we have excluded rapid rotators and very active stars.

After a further selection based on data quality (see next section), we obtained a final sample of 303 spectra of 230 stars. The sample includes 11 F-type stars, 56 G-type stars, 133 K-type stars and 30 M-type stars. The range in absolute magnitude covered is about $-5.4 \leq M_V \leq 9.0$. The most abundant are giant stars (about 50%) and main sequence stars (25%). The rest of the sample is represented by Class I, II and IV stars, about equally distributed.

3. Observations and data reduction

3.1. The IUE spectra

The IUE high resolution long wavelength spectra have been retrieved from the INES (IUE Newly Extracted Spectra) system through its Principal Centre at <http://ines.vilspa.esa.es>. A full description of the INES system for high resolution data is given in Cassatella et al. (2000) and González-Riestra et al. (2000). The spectra were inspected individually in the Mg II k region to identify and reject noisy and overexposed or underexposed data.

Representative examples which show the different typologies of the Mg II k profiles are given in Fig. 1. One can easily notice that the profiles differ significantly from case to case. The combined effects of the width of the emission line component, and of the strength and wavelength position of the absorption cause, quite frequently, the widths of the emission to be not directly measurable on the line profile itself.

We have then adopted a procedure which allows line widths to be evaluated in the large majority of cases. It is based on the reconstruction of the emission profile by fitting the observed portions of the emission line wings with a Gaussian function. Let the wavelength boundaries of the violet and red wings to be fitted be λ_1 to λ_2 and λ_3 to λ_4 , respectively. These wavelengths were determined manually from individual spectra and are indicated, in the order, with vertical bars in the examples of Fig. 1. The spectra were re-binned to increase the number of data points by a factor of 5, and slightly smoothed. After subtraction of the local continuum and normalization to the line peak emission, all spectra, irrespective of the typology of the profile were fitted with a Gaussian function. Line widths were defined as the full width of the *fitted* profile measured at half maximum of the *observed* line peak. This procedure is strictly needed for a correct evaluation of the line widths in the presence of strongly mutilated profiles, and is also useful in improving the accuracy of the line width measurements when dealing with noisy spectra. In the normal case of “well behaved” profiles such as c), d) and e) in Fig. 1, in which a direct measurement of the line width can be obtained from the spectra, the procedure provides

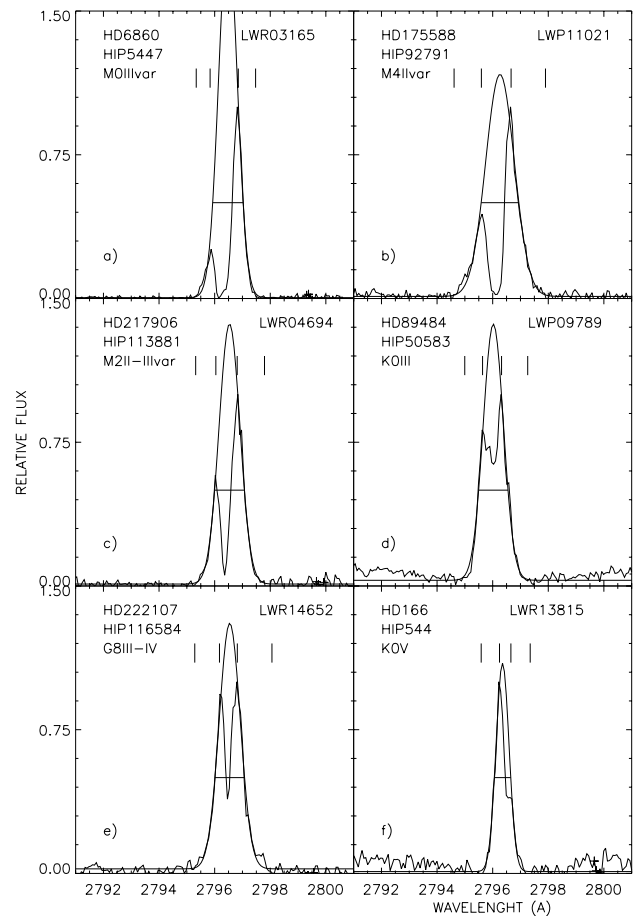


Fig. 1. Typical profiles of the Mg II k line. The vertical marks define the left and right wings of the emission line. The horizontal line indicates the *FWHM* of the profile.

values which are fully consistent, within the errors, with the ones obtained through the traditional methods.

Examples of extreme, although quite frequent cases in which a direct measurement using traditional methods cannot be done, are the profiles a) and b) of Fig. 1, in which the central absorption divides the profile in two unequal parts, the flux peak of one of them being less than 50% of the other, or in profiles of the type shown in panel f), in which one of the wings is mutilated by superimposed absorption (on the red wing in this case).

It should be stressed that, according to the numerical simulations by Cheng et al. (1997), the fluxes and profiles of chromospheric resonance lines depend on the temperature structure and dynamics of the atmosphere, which may inevitably lead to line profiles that are rather different from Gaussian. Our choice to use a Gaussian profile is just an empirical approach, having only to improve the accuracy of the line width measurements through a reliable reconstruction of the emission line wings. This procedure is particularly useful in the presence of severe intrinsic or interstellar line absorption.

As a general rule, the results of the fit were rejected whenever the peak intensity of the fitted profile exceeded the peak of the Mg II k observed profile by more than

a given amount, somewhat arbitrarily fixed to 180%. Also rejected were poor quality results where the relative error of the fit was larger than 10% (rms), and the results from strongly mutilated and asymmetric line profiles with a deep “central” absorption dividing the profile in two halves, with one having a peak intensity less than 10% of the other (i.e. similar to the limiting case a) of Fig. 1).

As for the errors on measured line widths, we have estimated it to be approximatively equal to half of the sampling interval of the spectra, corresponding to 3.64 km s^{-1} , for line profiles as in Figs. 1c–e, and twice this value for the other typologies.

The measured line widths W need to be corrected for instrumental broadening. Assuming the *IUE* Point Spread Function for high resolution spectra to be a Gaussian with a full width at half maximum $b = 18 \text{ km s}^{-1}$ at 2800 \AA (Evans & Imhoff 1985), the true width W_0 can be written as:

$$W_0^2 = W^2 - b^2. \quad (1)$$

This correction, which is especially important for narrow lines, has apparently not been taken into account in some previous works on the subject (see Sect. 4.4). Whenever multiple spectra were available for the same star, the line width was computed as the weighted mean of the individual measurements.

3.2. The Hipparcos data

For each of the 230 stars, the following information has been extracted from the Hipparcos Catalogue (ESA 1997): the Johnson V magnitude, the $B - V$ colour and the corresponding error, the parallax with its error, the spectral type and luminosity class, and information on variability or duplicity. In a few cases (suitably labeled in Table A, described below) the $B - V$ colour index, its error, and the spectral type were taken from the Strasbourg Data Center because the values contained in the *HIPPARCOS* catalogue were not considered reliable enough.

Table A¹ contains, for each object of the final sample, the HIP and HD numbers, the spectral type and luminosity class, the absolute magnitude M_V and its error $\sigma(M_V)$, the $B - V$ colour index with the corresponding error $\sigma(B - V)$, the *IUE* images used, the logarithm of the Mg II k line width $\log W_0$ with its error $\sigma(\log W_0)$. The absolute magnitudes were computed without any allowance for interstellar reddening. The errors in M_V have been derived from the errors in trigonometric parallaxes assuming a typical error of $\pm 0.01 \text{ mag}$ in the observed visual magnitudes.

The M_V vs. $B - V$ diagram of our sample of stars is shown in Fig. 2. One can easily recognize that main sequence stars with $B - V \geq 0.5$, as well as giant and supergiant stars, are well represented in our sample.

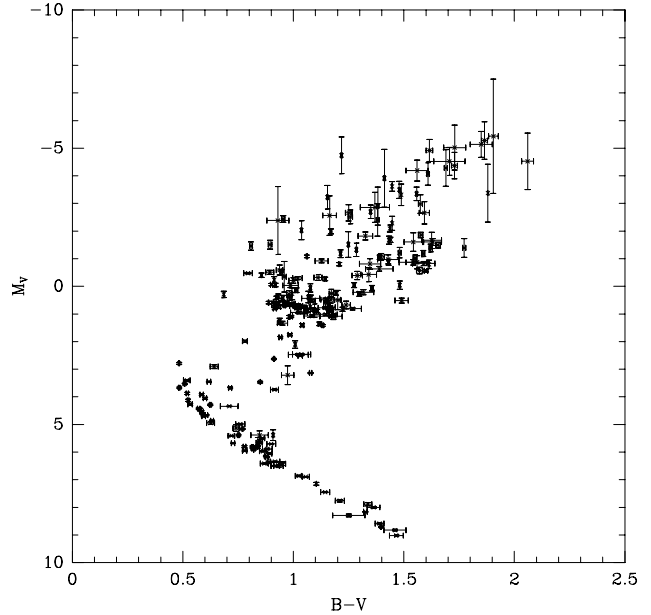


Fig. 2. Colour–magnitude diagram for the 230 stars in our sample.

4. Results

4.1. The present Mg II k width–luminosity relationship

To determine the coefficients a and b of the Mg II k Wilson–Bappu relationship

$$M_V = a + b \log W_0 \quad (2)$$

we applied linear regression algorithms to the M_V and $\log W_0$ data of the 230 stars in Table A. The numerical codes available from Press et al. (1992) were used.

We considered regression solutions which take into account the measurement errors in only one of the variables, as often done in the literature, or in both variables. Unweighted regression lines were also computed, although only for comparison purposes. In any case, the correlation coefficient between the M_V and $\log W_0$ data is $r = -0.94$.

The results obtained in the different cases are reported in Table 1. Column 1 contains the label assigned to the fit. In Col. 2 we specify the variable taken as independent. The variables for which the errors were taken into account are indicated in Col. 3. In particular, fits *A* and *B* were done without taking into account the measurement errors; in fits *C* and *D* only the errors on M_V or $\log W_0$ were considered, respectively; in the fits *E* and *F* the errors on both variables were taken into account. The regression coefficients a and b together with the corresponding errors are given in Cols. 4 and 5. They are consistently given in the format appearing in Eq. (2), even a switch of variables has been performed. In that case, the uncertainties on the coefficients have been accordingly propagated.

As shown in Table 1, the a and b coefficients derived by switching the independent variable ($\log W_0$ or M_V), vary significantly if allowance is made for the measurement errors in one variable only. This is the case of fit *C*, in which the independent variable is $\log W_0$ and only the errors on

¹ Table A is only available in electronic form at the CDS via anonymous ftp to cdsarc.u-strasbg.fr (130.79.128.5) or via <http://cdsweb.u-strasbg.fr/cgi-bin/qcat?J/A+A/374/1085>

Table 1. Coefficients of the Wilson–Bappu relationship.

FIT	I.V.	σ	a	b
A	$\log W_0$	none	29.54 ± 0.71	-14.37 ± 0.36
B	M_V	none	33.58 ± 0.84	-16.42 ± 0.41
C	$\log W_0$	M_V	28.42 ± 0.02	-13.44 ± 0.01
D	M_V	$\log W_0$	34.71 ± 0.18	-16.69 ± 0.09
E	$\log W_0$	both	34.56 ± 0.29	-16.75 ± 0.14
F	M_V	both	34.59 ± 0.29	-16.76 ± 0.14

Notes: Column 2, labeled I.V., specifies the variable, $\log W_0$ or M_V , taken as “independent variable”. Column 3, labeled σ , indicates for which of the variables the measurement errors were taken into account. The coefficients of the linear fit $M_V = a + b \log W_0$, together with the corresponding errors are given in Cols. 4 and 5. The correlation coefficient for all fits is $r = -0.94$.

M_V are taken into account, and fit *D*, in which the independent variable is M_V and only the errors in $\log W_0$ are taken into account. On the contrary, fits *E* and *F*, in which the errors on both variables are considered, provide fully consistent coefficients, irrespective of the variable considered as independent, as expected (Akritas & Bershadsky 1996).

The results in Table 1 show the important role played by the method used to analyse the data. This point is further discussed in Sect. 4.4.

We consider fit *E* or, equivalently, fit *F* in Table 1 as the most representative of the WB relationship, since the measurement errors on both variables were taken into account. In conclusion, the proposed WB relationship for the Mg II k line is:

$$M_V = (34.56 \pm 0.29) - (16.75 \pm 0.14) \log W_0. \quad (3)$$

The observed data, together with the corresponding error bars and the adopted WB relationship (labeled *E*) are shown in Fig. 3. For comparison, fit *C* is also shown (labeled *C*).

4.2. Dependence on effective temperature

We investigated the possible dependence of $\log W_0$ on stellar effective temperature, an item which has been addressed in previous recent analyses and is still under discussion.

Figure 4 shows our measurements of $\log W_0$ plotted as a function of the $B - V$ colour index, taken to be a temperature indicator. This representation is obviously equivalent to the colour–magnitude diagram in Fig. 2 by virtue of the Wilson–Bappu linear relationship. The figure shows, in particular, that $\log W_0$ is a decreasing function of $B - V$ for main sequence stars (indicated as black points), while it is an increasing function of $B - V$ for giants and supergiants (gray points on the upper part of the diagram). Therefore, the weak inverse relationship between line widths and stellar temperature found by SMW (see

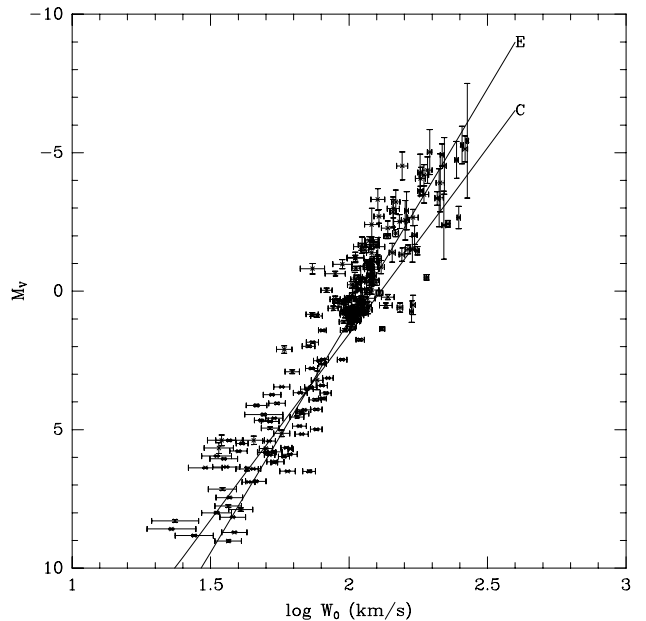


Fig. 3. The Wilson–Bappu effect in the Mg II k line for the 230 stars in our sample. The regression line labeled *E* corresponds to the proposed relationship in Eq. (3), obtained by taking into account the measurement errors on both variables. For comparison, the regression line *C* (see Table 1) is also provided, which has been obtained from the same data by taking into account only the errors on M_V .

their Fig. 5) simply reflects the distribution of their sample of stars in the HR diagram, which are mostly giants and supergiants.

An effective way to face the problem is to concentrate on stars in restricted ranges of M_V (so that any dependence on luminosity is taken out), and to compare their distribution in $B - V$ and in $\log W_0$. To start, we selected the stars having $-1.2 < M_V \leq -0.2$ (31 stars). The results, reported in Fig. 5, show clearly that $B - V$ is distributed over a wide range of values ($0.7 \leq B - V \leq 1.7$), while the distribution in $\log W_0$ has a very prominent peak around $\log W_0 = 2.05$. Line widths appear then to be substantially insensitive to the colour index, i.e. to the stellar effective temperature, at least in the above range of M_V . Tests made with stars lying in different ranges of M_V show a pattern which is similar to the one in Fig. 5, but the results cannot be considered as equally conclusive due to the paucity of stars available, and/or to the narrow $B - V$ range covered.

Using a different approach, previously followed by EEL, we investigated whether a different width–luminosity relationship applies to different spectral types. In Fig. 6, we compare our results of the width–magnitude relationships for G, K and M stars (solid lines) with the regression line corresponding to the full set of stars in our sample (Eq. (3); dashed line). The corresponding coefficients together with the number of stars used are given in Table 2. The fits were done by taking into account the errors on both variables. No attempt has been made to fit F–type star’s data, which are too few for a statistical approach.

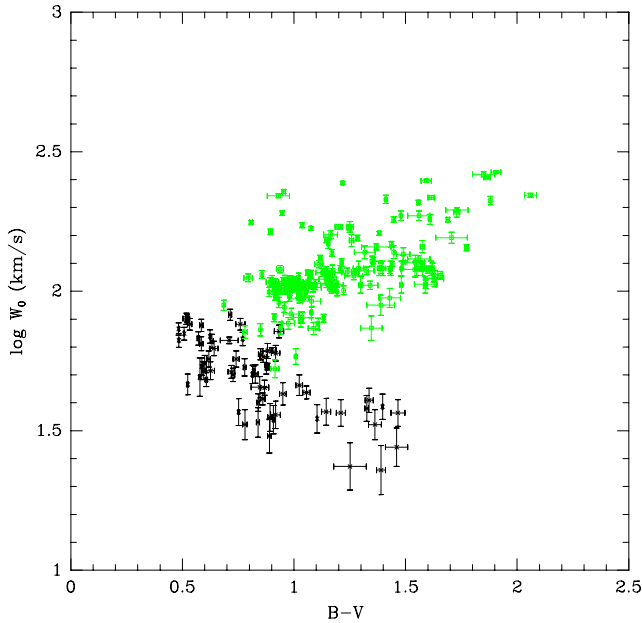


Fig. 4. Dependence of line width $\log W_0$ on $B - V$ for the stars in our sample. Black symbols refer to main-sequence stars and grey symbols to giant and supergiant stars.

In any case, not even better statistics could help in view of the intrinsically small range of M_V covered by F-type stars.

As it appears from Table 2, the coefficients for K-type stars (133 objects) are very similar to the ones in Eq. (3), as expected, given that these stars represent more than 50% of the entire sample.

The poorest statistics are those of M-type stars (30 objects), which are also unevenly distributed in M_V (see the gap $1 \leq M_V \leq 8$). Given these limitations, the WB coefficients are strongly dependent on the stars considered as input, so that the differences appearing from the table are not significant enough.

As for G-type stars (56 objects), we find a significantly flatter slope than for K-type stars (133 objects). In particular, the line widths of the G-type stars in Fig. 6 with $M_V \leq -1$ are broader than one would expect from the WB relation in Eq. (3). A similar trend has been reported by EEL for a sample of 22 G-type stars. In this regard, it is interesting to mention that Wallerstein et al. (1999), in their study of the WB effect in the Ca II k line, also found a group of luminous G-type stars having substantially broader Ca II lines than predicted by the WB relation. Whether the apparently different WB relation for G-type stars should be regarded as a true temperature effect as claimed by EEL, or is due to other causes (including selection effects), cannot be clarified at this stage.

4.3. Dependence on metallicity

We investigated possible departures from the Wilson–Bappu relationship in Eq. (3) due to a dependence of the Mg II k line width on metallicity. To this purpose, we

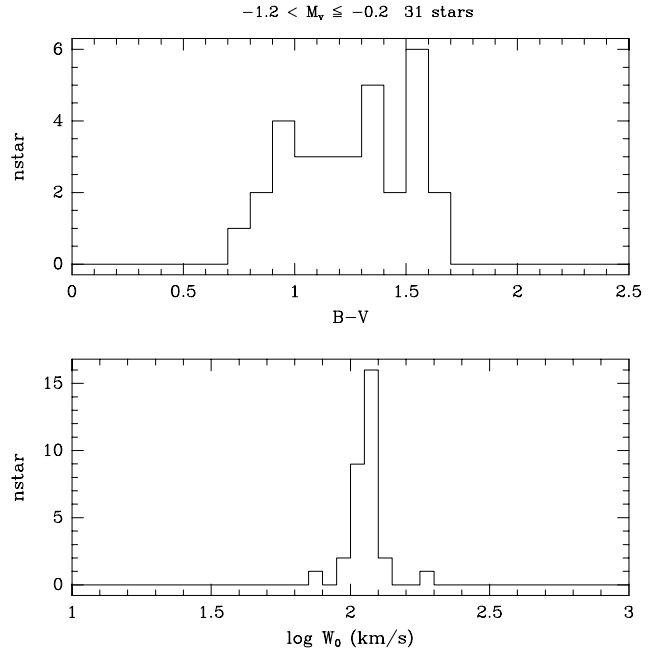


Fig. 5. Histogram of $B - V$ (top) and $\log W_0$ for stars in a restricted range of absolute magnitude $-1.2 < M_V \leq -0.2$ (31 stars).

Table 2. Coefficients of the fit for different spectral types.

Sp. Type	N	a	b	r
G-stars	56	28.82 ± 0.42	-13.88 ± 0.20	-0.91
K-stars	133	36.94 ± 0.41	-17.93 ± 0.20	-0.93
M-stars	30	31.77 ± 1.22	-15.63 ± 0.58	-0.96

Notes: Columns 1 to 5 give, in order, the spectral type considered, the number of stars used, the regression coefficients with the corresponding errors, and the linear correlation coefficient.

looked for [Fe/H] literature data and found information for 156 stars of our sample. For 12 stars, the [Fe/H] values are from Carney et al. (1994), and for the remaining stars from Cayrel de Strobel et al. (1997). This latter being a compilation from several sources, more than one determination was in general available for a given star. In these cases, the most recent one has been adopted, and assumed to be the most reliable. In Fig. 7 we plot as a function of [Fe/H] the difference $\Delta \log W_0$ between the measured line width $\log W_0$ and the value expected from the Wilson–Bappu relationship in Eq. (3). It clearly appears from the figure that, in spite of the quite large range in metallicity, there is no trend for the line widths to show any systematic deviation. The correlation coefficient between [Fe/H] and the deviations $\Delta \log W_0$ from Eq. (3) is indeed very poor: $r = 0.16$.

As a further confirmation of this point, we divided the 156 stars into four groups according to their metallicity. For each group we made a linear fit of M_V as a function of $\log W_0$ (allowing for the errors on both

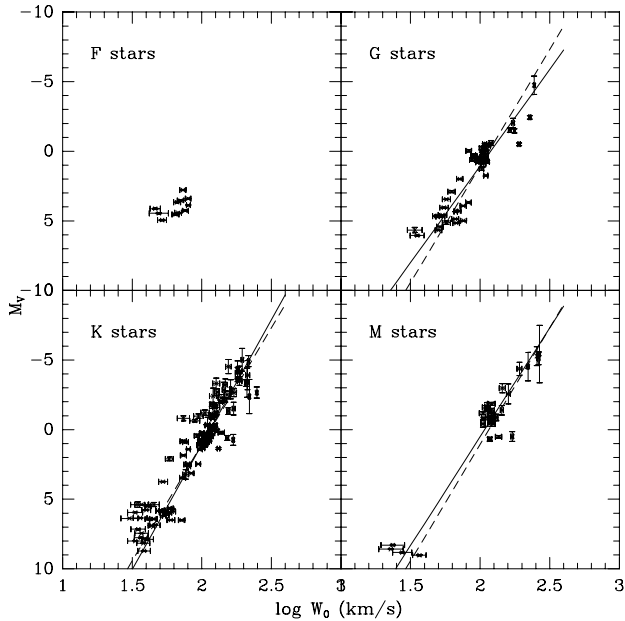


Fig. 6. The Wilson–Bappu relationship for different spectral types.

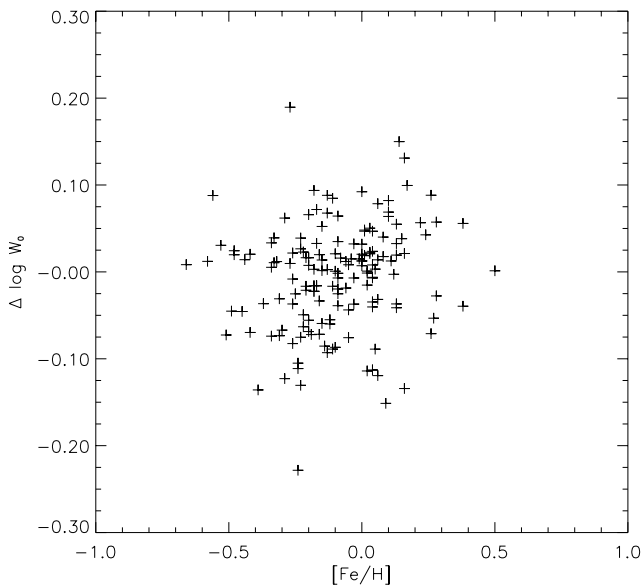


Fig. 7. The departure of the observed line width $\log W_0$ with respect to the Wilson–Bappu relationship in Eq. (3) is plotted as a function of metallicity $[\text{Fe}/\text{H}]$ for 156 stars in our sample.

variables). The metallicity groups were defined as follows: $\log[\text{Fe}/\text{H}] \leq -0.3$ (23 stars), $-0.3 < \log[\text{Fe}/\text{H}] \leq -0.1$ (56 stars), $-0.1 < \log[\text{Fe}/\text{H}] \leq +0.1$ (54 stars), and $\log[\text{Fe}/\text{H}] > +0.1$ (23 stars). Slightly different slopes and intercepts of the WB relationship were found, but no dependence on metallicity was found.

4.4. Comparison with previous determinations

The results of the present study are compared with the literature values of EEL and SMW in Table 3 which gives, for each author, the number of stars used, the coefficients a

Table 3. Comparison with previous results.

Reference	N	a	b	M_V range
Eq. (3) (Fit E)	230	34.56 ± 0.29	-16.75 ± 0.14	-5.4 9.0
Fit C	230	28.42 ± 0.02	-13.44 ± 0.01	-5.4 9.0
EEL 1999	65	35.25 ± 2.17	-17.61 ± 1.10	-5.1 12.3
SMW 1998	92	28.63	-13.53	-2.2 7.5

Notes: EEL and SMW stand for Elgarøy et al. (1999) and Scoville & Mena–Werth (1998), respectively. Column 2 provides the number of stars used by the different authors. Fits *E* (the proposed WB relationship) and *C* are the same as in Table 1.

and b (with their errors, if available), and the range of M_V values from which the WB relationship has been derived. Reference is made only to papers making use of the same definition of line width ($FWHM$ in this case), and based on precise *HIPPARCOS* parallaxes.

Since our sample contains 84 stars in common with SMW and 34 in common with EEL, it is useful to make a direct comparison between the line width measurements.

As it appears from the top panel of Fig. 8, our measurements of W_0 are in a good agreement with SMW’s values for the broadest lines, but there is an increasing discrepancy for narrower and narrower lines, whose widths are systematically overestimated by SMW, as would happen if their measurements were not corrected for the instrumental width (Eq. (1)), an item which is not specified in their paper. Compared with ours, the SMW’s measurements of W are about 8% higher, on average. In spite of this discrepancy, one can see from Table 3 that SMW’s fit is very close to our fit *C*, but differs strongly from the others. This might suggest that it has been obtained by weighting only on M_V , as fit *C*.

The agreement with EEL’s measurements of W (Fig. 8, bottom panel) is substantially better, amounting to 2%, if 4 discrepant data points are excluded (note that for such a comparison, we have averaged the two determinations of W obtained by EEL with different methods – see their Table 1). As one can easily appreciate from Table 3, our best estimate of the WB effect in Eq. (3) is compatible with EEL’s fit, at least within their large error bars. Unfortunately, no information about the treatment of measurement errors is given by EEL. The only authors who declared to have taken the measurement errors on both variables into account are Vladilo et al. (1987), but their results cannot be compared with ours due to their much more limited range in M_V (-1 to 7). We should note also that the values of M_V here adopted coincide with those of SMW, while there is, on average, a systematic difference of 0.12 mag, of unknown origin, between EEL’s values of M_V and ours.

In conclusion, given the substantially larger amount of observations analysed in this work, and the proper way to take the measurement errors into account, we consider Eq. (3) to adequately represents the WB effect for the

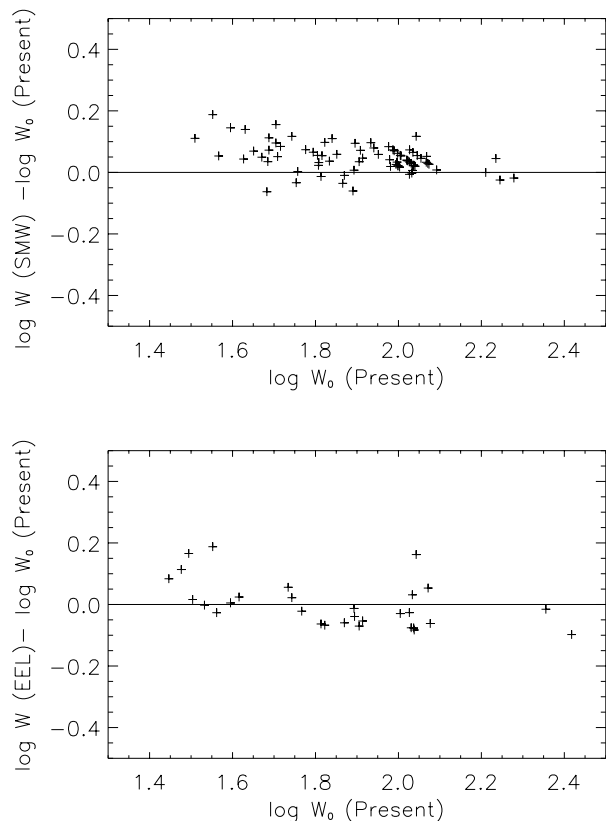


Fig. 8. Comparison of our line width measurements with those of Scoville & Mena–Werth (1998; labeled SMW) and of Elgarøy et al. (1999; labeled EEL).

Mg II k line, at least within the observational limits set by the *IUE* and *HIPPARCOS* experiments.

5. Conclusions

In this paper we provide an accurate Wilson–Bappu relationship for the Mg II k line (see Eq. (3)) based on *IUE* and *HIPPARCOS* observations, which can be used to estimate stellar distances over a wide range of absolute magnitudes: $-5.4 \leq M_V \leq 9.0$. The sample of stars (230 objects) is considerably larger than the ones used in previous works.

It has been shown that the coefficients of the WB relationship critically depend upon the choice of the method of analysis. In our case, different fitting algorithms have been tested and the one taking into account the measurement errors on both variables has been adopted as the most suitable.

In spite of the more accurate method and of the wider sample of stars used, we have not found any observational confirmation to the claimed dependence of the WB effect on effective temperature. On the contrary, we have found arguments against such an effect, such as the one provided in the histograms in Fig. 5, which show that the Mg II line width is substantially the same for stars in a narrow range of M_V ($-1.2 < M_V \leq -0.2$), in spite of the wide range of $B - V$ values. In any case, on the basis of theoretical

considerations, the temperature effect is expected to be small (Reimers 1973; Özeren et al. 1999).

We also investigated possible systematic deviations caused by differences in metallicity. Using metallicity data for 156 stars in our sample, we came to the conclusion that such an effect is not present, at least within the accuracy of the measurements.

Given the difficulty of disentangling the metallicity and temperature effects using the present sample of field stars, it would be important to extend the analysis to homogeneous populations of stars such as galactic clusters. In general, observations by newly proposed space missions (e.g. GAIA) will hopefully enrich our knowledge on parallaxes of very large numbers of stars and clarify the problems left open.

Acknowledgements. We would like to thank Prof. M. J. Fernández-Figueroa and Drs. Anna Marenzi, Vittoria Caloi, and R. González-Riestra for useful comments and advice.

References

- Akritas, M. G., & Bershady, M. A. 1996, *ApJ*, 470, 706
Cassatella, A., Altamore, A., González-Riestra, R., et al. 2000, *A&AS*, 141, 331
Cassatella, A., Holm, A., Reimers, D., Ake, T., & Stickland, D. J. 1985, *MNRAS*, 217, 589
Cayrel de Strobel, G., Soubiran, C., Friel, E. D., Ralite, N., & Francois, P. 1997, *A&AS*, 124, 299
Carney, B. W., Latham, D. W., Laird, J. B., & Aguilar, L. A. 1994, *AJ*, 107, 2240
Cheng, Q. Q., Engvold, O., & Elgarøy, Ø. 1997, *A&A*, 327, 1115
Elgarøy, Ø. 1988, *A&A*, 204, 147
Elgarøy, Ø., Joras, P., Engvold, O., et al. 1988, *A&A*, 193, 211
Elgarøy, Ø., Engvold, O., & Lund, N. 1999, *A&A*, 343, 222
Gillet, D., Ferlet, R., Maurice, E., & Bouchet, P. 1985, *A&A*, 150, 89
García-Alegre, M. C., Ponz, J. D., & Vásquez, M. 1981, *A&A*, 96, 17
González-Riestra, R., Cassatella, A., Solano, E., Altamore, A., & Wamsteker, W. 2000, *A&AS*, 141, 343
ESA 1997, *The Hipparcos and Tycho Catalogues*, ESA SP-1200
Evans, N. R., & Imhoff, C. L. 1985, *NASA IUE Newsletter*, 28, 77
Kraft, R. P. 1960, in *Stars and Stellar Systems*, vol. VI, ed. J. L. Greenstein (Univers. of Chicago Press), 401
Montes, D., Fernández-Figueroa, M. J., De Castro, E., & Cornide, M. 1994, *A&A*, 285, 609
Özeren, F. F., Doyle, J. G., & Jevremovic, D. 1999, *A&A*, 350, 635
Press, W. H., Teukolsky, S. A., Vetterling, W. T., & Flannery, B. P. 1992, *Numerical Recipes* (Cambridge Univ. Press)
Reimers, D., & Cassatella, A. 1985, *ApJ*, 297, 275
Reimers, D. 1973, *A&A*, 24, 79
Vladilo, G., Molaro, P., Crivellari, L., et al. 1987, *A&A*, 185, 233
Scoville, F., & Mena–Werth, J. 1998, *PASP*, 110, 794
Wallerstein, G., Machado-Pelaez, L., & Gonzalez, G. 1999, *PASP*, 111, 335
Wilson, O. C., & Bappu, M. K. V. 1957, *ApJ*, 125, 661